Latin American Journal of Solids and Structures
www.lajss.org

# Impact Response of Functionally Graded Conical Shells

**Abstract**

This paper presents low velocity impact response of functionally graded pretwisted conical shells. The modified Hertzian contact law which accounts for permanent indentation is utilized to compute the contact force and other impact parameter. The time dependent equations are solved by Newmark's time integration scheme. An eight noded isoparametric quadratic element is employed in the present finite element formulation. A parametric study is carried out to investigate the effects of triggering parameters like initial velocity of impactor, twist angle, oblique impact angle, location of impact for Stainless Steel-Nickel functionally graded conical shell subjected to low velocity impact.

**Keywords**

functionally graded material; finite element; low velocity impact; twist angle; oblique impact angle; conical shell

**Sudip Dey** [a]
**Sondipon Adhikari** [b]
**Amit Karmakar** [c]

[a] Swansea University, United Kingdom, email: infosudip@gmail.com (corresponding author)
[b] Swansea University, United Kingdom [c] Jadavpur University, Kolkata, India

http://dx.doi.org/10.1590/1679-78251382

Received 27.05.2014
In revised form 28.09.2014
Accepted 06.10.2014
Available online 13.10.2014

## 1 INTRODUCTION

Functionally graded materials (FGM) have gained immense popularity as advanced engineering materials due to its high corrosion and heat resistance properties along with high strength and stiffness. Such materials are the novel inhomogeneous materials consisting of a mixture of isotropic materials in which the material properties are graded but continuous particularly along a given direction to improve the quality of performance. In general, these materials are made from a mixture of ceramic and metal to take the advantage of the desirable properties such as heat and corrosion resistance of ceramics and high toughness, tensile strength and bonding capability of metals. Functionally graded shallow conical shells could be idealized as rotating turbomachinery blades which could be employed in aerospace, nuclear and mechanical industries. Functionally graded materials have been increasingly used in design of impact resistant structures as well as in design of advanced thermal barrier coatings. A plate with a functionally graded layer from ceramic to metal through its thickness combines the superior features of ceramic and metal. Thus, the ceramic-rich side provides good protection against projectiles while the metal rich side offers toughness and strength to main-

tain the integrity of the structure as long as possible. Hence, for the purpose of design and manufacturing, the accurate evaluation of their low velocity impact response behaviour of such FG conical shell is important for the designers to ensure the operational safety. The pioneering investigations on FGMs for the low velocity impact analysis were carried out by Goldsmith (1960) and Abrate (1998). Several studies on low velocity impact is carried out in past last two decades but mostly on composite structures. Shariyat and Farzan Nasab (2014) studied the low-velocity impact analysis of the hierarchical viscoelastic FGM plates using an explicit shear-bending decomposition theory and the new differential Quadrature method, while previously Yalamanchili and Sankar (2012) investigated on indentation of functionally graded beams and its application to low-velocity impact response.

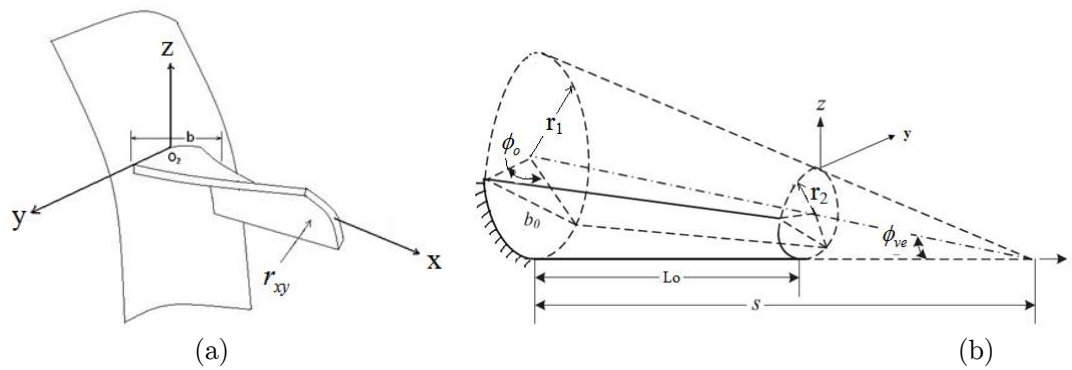


Figure 1: (a) Pretwisted turbo-machinery blade (b) Conical shell model.

## Nomenclature

| | |
|---|---|
| $C_i$ | Material property |
| $V_f$ | Volume fraction |
| $N$ | Material property graded index (or Power law exponent) |
| $t$ | Thickness |
| $E$, $G$, $\upsilon$ | Young's modulus, Shear modulus and Poisson's ratio, respectively |
| $\varrho$ | Mass density |
| $r_1$ , $r_2$ | Radius of curvature ($r_2 < r_1$) |
| $r_x$ , $r_y$ | Radius of curvature in x-direction and y-direction, respectively |
| $r_{xy}$ | Radius of twist |
| Lo, bo | Length,Reference width |
| $\phi_{ve}$ | Vertex angle |
| $\phi_o$ | Base subtended angle of cone |
| [M] | Global mass matrix |
| [K] | Global elastic stiffness matrix |
| {F} | Global vector of externally applied load |
| {δ} | Global displacement vector |
| ς, χ | Local natural coordinates of the element |

| | |
|---|---|
| x, y, z | Local coordinate axes (plate coordinate system) |
| Lo/s | Aspect ratio |
| $F_C$ | Contact force |
| V | Impactor's velocity |
| $\alpha$ | Local indentation |
| $\alpha_m$ | Maximum local indentation |
| $\Delta t$ | time step |
| $k_{modified}$ | Modified contact stiffness |
| VOI | Initial velocity of impactor |
| $\psi$ , $\beta_i$ | Twist angle and oblique impact angle, respectively |
| D/t | Deflection/thickness (non-dimernsional) |
| ID | Impactor's displacement |
| VOI | Initial velocity of impactor |

However, to the best of authors' knowledge, the available works regards to the low velocity impact analysis of FGM is mostly to functionally graded plates [Khalili et al. (2013) Gunes, 2014)]. Kiani et al. (2013) studied on low velocity impact response of thick FGM beams with general boundary conditions in thermal field while Eghtesad et al. (2012) studied the dynamic behavior of ceramic–metal FGM under high velocity impact conditions using corrective smoothed particle algorithm (CSPM) method. In contrast, Mao et al. (2011, 2013) analyzed the nonlinear dynamic response for functionally graded shallow spherical shell under low velocity impact in thermal environment and also investgated on interfacial damage analysis of shallow spherical shell with FGM coating under low velocity impact. Amirhossein et al. (2011) studied on transient analysis of functionally graded cylindrical shell under impulse local loads while 3D finite element simulation of sandwich panels with a functionally graded core subjected to low velocity impact was investigated by Etemadi et al. (2009) and subsequently for sandwich beams with functionally graded core was studied by Apetre et al. (2006). On the other hand, Kubair and Lakshmana (2008) modelled the low-velocity impact damage in layered functionally graded beams. Much effort has been devoted to various structural analyses of functionally graded structures, such as thermal stresses, static, buckling, and vibration analyses. Remarkable investigation is also carried out by Fukui et al. (1993), Praveen and Reddy (1998) and Noda (1999). However, Karmakar and Kishimoto (2006) conducted the transient dynamic response of delaminated composite rotating shallow shells subjected to impact. Of late, Shariyat and Jafari (2013) studied semi-analytical low-velocity impact of bidirectional FG circular plates while Shariyat and Farzan (2013) investigated on nonlinear eccentric low-velocity impact analysis of a highly prestressed FGM rectangular plate by using a refined contact law.

In present study, Stainless Steel-Nickel functionally graded material is investigated to address the effects of the twist angle, volume fraction, initial velocity of impactor and location of impact, on transient dynamic response subjected to low velocity impact. To bridge the research gap identified in the open literature review, the effect of low velocity impact response analysis of the functionally graded conical shells is studied. To the best of the authors' knowledge and considering the review of the open literature, it is revealed that the combined effect of oblique impact and twist on functionally graded shallow conical shell structure has not received due attention. To fill up this apparent

void, the present study employed a finite element based numerical approach to study the low velocity impact analyses of pretwisted functionally graded shallow conical shells. The finite element analyses are carried out using an eight-noded isoparametric quadratic element considering the effects of triggering parameters like the twist angle, location of impact, oblique impact angle.

## 2 GOVERNING EQUATIONS

Functionally graded materials (FGM) are defined as the combination of two or more materials. If 'C' denotes a function of the material properties and volume fractions of the constituent materials, it can be expressed as (Zhao and Liew, 2011)

$$C = \sum_{i=1}^{k} C_i \quad V_{fi} \tag{1}$$

Where the material property ($C_i$) and volume fraction ($V_f$) of the constituent material '$i$'. The material properties of the functionally graded conical shells vary continuously and smoothly across the thickness of FG conical shell. Without loss of generality of the formulation and the method of solution, in this study the effective material properties are obtained using the power law distribution (Loy et al., 1999),

$$E(t) = E_m + (E_c - E_m)\left[\frac{(2w+t)}{2t}\right]^N \tag{2}$$

$$\nu(t) = \nu_m + (\nu_c - \nu_m)\left[\frac{(2w+t)}{2t}\right]^N \tag{3}$$

$$\rho(t) = \rho_m + (\rho_c - \rho_m)\left[\frac{(2w+t)}{2t}\right]^N \tag{4}$$

where E, υ and ρ denote Young's modulus, Poisson's ratio and mass density with suffix as 'c' and 'm' indicating the corresponding values at the outer surface (ceramic rich) and inner surface (metal rich) of functionally graded conical shell. A functionally graded conical shell panel is shown in Fig. 1, where a coordinate system (x, y, z) is established on the middle surface of the conical shell panel. The geometric properties of the conical shell are represented by length Lo, semi-vertex angle $\phi_{ve}$, base subtended angle $\phi_o$, thickness t, and the radii at the two ends $r_1$ and $r_2$ ($r_1 > r_2$). In the spanwise direction of FG conical shell, no curvature is considered (i.e., $r_x=\infty$). The cone radius at any point along its length is given by

$$r_y(z) = r_2 - z\,Sin(\phi_{ve}/2) \tag{5}$$

In general, a shallow shell is characterized by its middle surface which is defined by the equation,

$$z = -0.5\,[(x^2/r_x) + (2xy/r_{xy}) + (y^2/r_y)] \tag{6}$$

The radius of twist ($r_{xy}$), length ($Lo$) of the shell and twist angle ($\Psi$) are expressed as (Liew et al., 1994),

$$r_{xy} = -Lo/\tan\psi \tag{7}$$

## 3 MODIFIED CONTACT LAW

The modified Hertzian contact law which accounts for permanent indentation is utilized to compute the contact force between the impactor and the shallow conical shells. Larson and Palazotto (2006) proposed a modified contact force stiffness which accounts for the graded profile of the FGM media through the thickness. The impactor is modelled as an elastic solid. The contact force is assumed to be a point load and impact surface of impactor is considered to be spherical. During loading-unloading cycle, the contact force can be evaluated as (Sun and Chen, 1985),

$$F_C = k_{modified}\,\alpha^{1.5} \qquad 0 < \alpha \leq \alpha_m \tag{8}$$

where $\alpha$ is the local indentation i.e., change in distance between centre of the impactor and the mid-surface of target shell and $\alpha_m$ is the maximum local indentation. The modified contact stiffness of the Hertzian contact theory employed as [Larson and Palazotto (2006) and Shariyat and Farzan Nasab (2014)],

$$k_{modified} = \frac{16}{3\pi}\,\frac{1}{k_{target} + k_{impactor}}\sqrt{\frac{C_r}{\lambda}} \tag{9}$$

where $\lambda$ is a constant depending on the shape of impactor and target. In case of low velocity impact, the value of this constant $\lambda$=2 is chosen which depends on contact behavior between a conical shell target and a spherical impactor. Besides, $C_r$ is a constant depending on the curvatures of both impactor and projectile and is expressed as,

$$\frac{1}{C_r} = \frac{1}{r_1^{impactor}} + \frac{1}{r_2^{impactor}} + \frac{1}{r_1^{target}} + \frac{1}{r_2^{target}} \tag{10}$$

For spherical impactor, the principal radii are equal (i.e., $r_1 = r_2$). The dynamic equilibrium equation for moderate rotational speeds neglecting Coriolis effect is derived employing Lagrange's equation of motion in global form (Dey and Karmakar, 2012)

$$[M]\{\delta''\} + [K]\{\delta\} = \{F\} \tag{11}$$

where $\{\delta\}$ is global displacement vector. For the impact problem, $\{F\}$ is given as

$$\{F\} = \{0\ 0\ 0 \ldots\ldots F_C \ldots\ldots 0\ 0\ 0\}^T \tag{12}$$

where $F_C$ is the contact force and the equation of motion of the rigid impactor is obtained as,

$$m_i\,\omega''_i + F_C = 0 \tag{13}$$

where $m_i$ and $\omega''_i$ are mass and acceleration of impactor, respectively. The time dependent equations are solved by Newmark's integration scheme (Bathe, 1990). The local indentation is formulated as (Karmakar and Sinha, 1998)

$$\alpha(t) = w_i(t)\ \mathrm{Cos}\ \beta i - w_p\ (x_c,\ y_c,\ t)\ \mathrm{Cos}\psi \tag{14}$$

where $w_i$ and $w_p$ are impactor's displacement (ID) and target plate displacement along global z direction at the impact point $(x_c,\ y_c)$, respectively. Both normal impact and oblique impact by a spherical mass on functionally graded conical shell at central point is shown in Figure 2. Here $\psi$ and $\beta_i$ are the twist angle and the oblique impact angle, respectively. The components of force at the impact point in global directions are given by

$$F_{ix} = 0,\ \ F_{iy} = F_C\ \mathrm{Sin}\psi,\ \ F_{iz} = F_C\ \mathrm{Cos}\psi \tag{15}$$

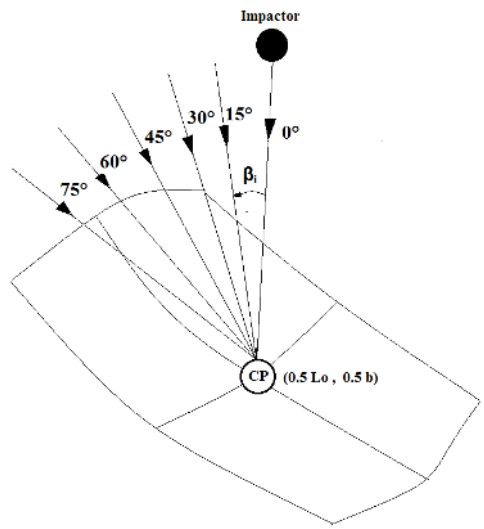


Figure 2: Impact (normal and oblique) on FG conical shell by a spherical mass at centre

## 4 FINITE ELEMENT FORMULATION

An eight noded isoparametric quadratic element with five degrees of freedom at each node (three translation and two rotations) is employed wherein the shape functions ($S_i$) are as follows (Bathe, 1990)

$$S_i = (1 + \chi\,\chi_i)\ (1 + \varsigma\,\varsigma_i)\ (\chi\,\chi_i + \varsigma\,\varsigma_i - 1)\ /\ 4 \qquad (\text{for } i = 1, 2, 3, 4) \tag{16}$$

$$S_i = (1 - \chi^2)\ (1 + \varsigma\,\varsigma_i)\ /\ 2 \qquad (\text{for } i = 5, 7) \tag{17}$$

$$S_i = (1 - \varsigma^2)\ (1 + \chi\,\chi_i)\ /\ 2 \qquad (\text{for } i = 6, 8) \tag{18}$$

where $\varsigma$ and $\chi$ are the local natural coordinates of the element. Here $\chi_i = +1$ for nodes 2, 3, 6 and $\chi_i = -1$ for nodes 1, 4, 8 and $\varsigma_i = +1$ for nodes 3, 4, 7 and $\varsigma_i = -1$ for nodes 1, 2, 5 as furnished in Fig.

3. The correctness of the shape functions is checked from the relations

$$\sum_{i=1}^{8} S_i = 1, \qquad \sum_{i=1}^{8} \frac{\partial S_i}{\partial \varsigma} = 0, \qquad \sum_{i=1}^{8} \frac{\partial S_i}{\partial \chi} = 0 \tag{19}$$

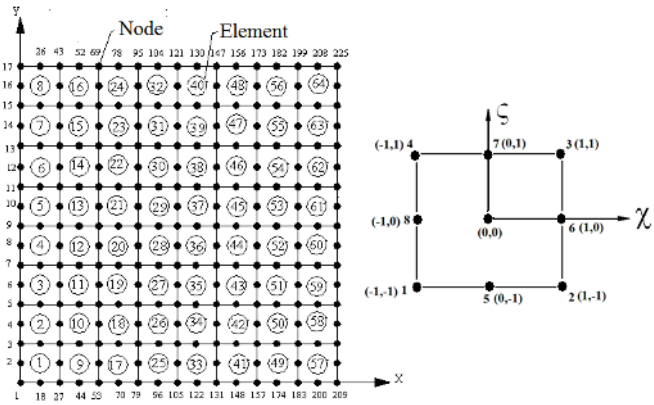


Figure 3: A typical discretisation of 8 x 8 mesh on plan area with element, node numbers and the natural coordinates of an isoparametric quadratic element.

In an isoparametric quadratic element formulation, the generalized displacements and co-ordinates are interpolated from their nodal values by the same set of shape functions. Hence, the co-ordinates (x, y) of any point within an eight-noded element are obtained as

$$x = \sum_{i=1}^{8} S_i \, x_i \qquad y = \sum_{i=1}^{8} S_i \, y_i \tag{20}$$

The relations between the displacement $(u,v,w,\vartheta_x,\vartheta_y)$ at any point with respect to the coordinates $(\varsigma, \chi)$ and nodal degrees of freedom are expressed as

$$u = \sum_{i=1}^{8} S_i \, u_i \,, \quad v = \sum_{i=1}^{8} S_i \, v_i \,, \quad w = \sum_{i=1}^{8} S_i \, w_i \,, \quad \theta_x = \sum_{i=1}^{8} S_i \, \theta_{xi} \,, \; \theta_y = \sum_{i=1}^{8} S_i \, \theta_{yi} \tag{21}$$

and $$\begin{bmatrix} S_{i,x} \\ S_{i,y} \end{bmatrix} = [J]^{-1} \begin{bmatrix} S_{i,\varsigma} \\ S_{i,\chi} \end{bmatrix} \text{ where } [J] = \begin{bmatrix} x_{,\varsigma} & y_{,\varsigma} \\ x_{,\chi} & y_{,\chi} \end{bmatrix} \text{ is the Jacobian matrix.} \tag{22}$$

Based on the first-order shear deformation theory, the displacement field of the conical shell may be described as

$$\begin{aligned} u(x, y, z) &= u^0(x, y) - z\, \vartheta_x (x, y) \\ v(x, y, z) &= v^0(x, y) - z\, \vartheta_y (x, y) \\ w(x, y, z) &= w^0(x, y) = w(x, y) \end{aligned} \tag{23}$$

where, $u^0$, $v^0$, and $w^0$ are displacements of the reference plane of the plate, and $\vartheta_x$ and $\vartheta_y$ are rotations of the cross section relative to x and y axes, respectively. Hamilton's principle (Meirovitch, 1992) applicable to non-conservative system can be expressed as,

$$\delta H = \int_{t_1}^{t_2} [\delta T - \delta U - \delta W] dt = 0 \tag{24}$$

where T, U and W are total kinetic energy, total strain energy and total potential of the applied load, respectively wherein δW=0 for free vibration analysis. The Lagrange's equation of motion is given by

$$\frac{d}{dt}\left[\frac{\partial L_f}{\partial \delta_e}\right] - \left[\frac{\partial L_f}{\partial \delta_e}\right] = \{F_e\} \tag{25}$$

where $\{F_e\}$ is the applied external force vector of an element and $L_f$ is the Lagrangian function. Substituting $L_f = T - U$ in Lagrange's equation incorporating the corresponding expressions for T and U, the dynamic equilibrium equation for each element in the following form

$$[M_e]\{\ddot{\delta}_e\} + [K_e]\{\delta_e\} = \{F_e\} \tag{26}$$

where $\{\delta_e\}$ is the element displacement vector, $[M_e]$ is the element mass matrix, $[K_e]$ is the element stiffness matrix, $\{F_e\}$ is the element force vector. After assembling all the element matrices and the force vectors with respect to common global coordinates, the resulting equilibrium equation of the structure becomes the form of equation (11).

## 5 RESULTS AND DISCUSSION

Parametric studies are carried out with respect to twist angle, location of impact, oblique impact angle on low velocity impact response behaviour of functionally graded shallow conical shells. Material properties of functionally graded materials [Zhao and Liew (2011) and Loy et al. (1999)] are adopted as stipulated in Table 1. Even though the main application of functionally graded material is in the area of thermal field where the temperature gradient is significantly high, the present study is addressed to the combined effect of twist and impact response (both normal and oblique) on the the functionally graded conical shell which is idealized as turbomachinery blade. The constant uniform temperature (300 K) is considered as the temperature of the blade as a representative investigation during engine start up (i.e., at the beginning from uniform room temperature) and the blade is gradually exposed to the operational external environment.

| Material | E $(N/m^2)$ | υ | ρ $(Kg/m^3)$ |
|---|---|---|---|
| Stainless Steel (SS) | $207.788 \times 10^9$ | 0.317756 | 8166 |
| Nickel (Ni) | $205.098 \times 10^9$ | 0.310000 | 8900 |
| Aluminum (Al) | $70.000 \times 10^9$ | 0.300000 | 2707 |
| Zirconia ($ZrO_2$) | $151.000 \times 10^9$ | 0.300000 | 3000 |

Table 1: Properties of the FGM components at 300 K.

The results obtained from the computer code developed on the basis of present finite element modelling are validated with those in the literature in respect of low velocity impact [Goldsmith (1960) and Kiani et al. (2013)]. To validate the present finite element formulation in respect of impact response, computation has been carried out for flat isotropic and laminated plates. In this context, essentially two important aspects namely, analytical solution and finite element treatment have been taken into account. The results of Goldsmith (1960) are compared considering a simply supported 0.2 m square and 0.008 m deep steel plate impacted centrally by a steel sphere of 0.01 m radius with initial velocity of 1.0 m/sec which provides solution of an integral equation for a Hertzian type of contact law in which the contact force is expressed as

$$F_c = K_o \, \alpha^{3/2}$$

$$\text{where} \quad K_o = \frac{4}{3\pi}\sqrt{R_{imp}}\,\left(\frac{1}{\delta_1+\delta_2}\right), \quad \delta_1 = \frac{(1-\upsilon_1^2)}{E_1\pi}, \quad \delta_2 = \frac{(1-\upsilon_2^2)}{E_2\pi}$$

Here $R_{imp}$ is the impactor's radius and $K_o$ is the contact stiffness. The material parameters considered as $E_1 = E_2 = E_i = 200$ GPa, $G_{12} = G_{23} = G_{13}$=77 GPa, $\rho$=7800 kg/m$^3$, $\nu_i$=$\nu_{12}$= 0.3 and the time step chosen is 1.0 μ-sec with corresponding finite element mesh of (8 x 8) for full plate. Figure 4 depicts the comparisons of time histories of contact force, central deflection of target plate, impactor's displacement and velocity obtained from present FEM and that of Goldsmith (1960). The slight discrepancies in the present results can be attributed to the fact that the effect of rotary inertia and transverse shear deformation were neglected by Goldsmith but the nature of variation is same. In Figure 5, the time histories of contact force are validated for Silicon Nitride and Stainless Steel functionally graded beam as analyzed by Kiani et al. (2013) using Ritz method, while the tiny discrepancies in the results with those of Kiani et al. (2013) could be attributed to the fact that as the Ritz method overestimates the impact parameter as a consequences of the material property graded index increases wherein the indentation parameter increases which is expected since beam becomes softer as power law index increases up. Moreover, the properties of each homogeneous layer are considered as the average of the properties at the top and bottom surfaces of each layer, hence, the number of layers, for sure affects the contact force, time step and indentation parameters in case of Ritz method.

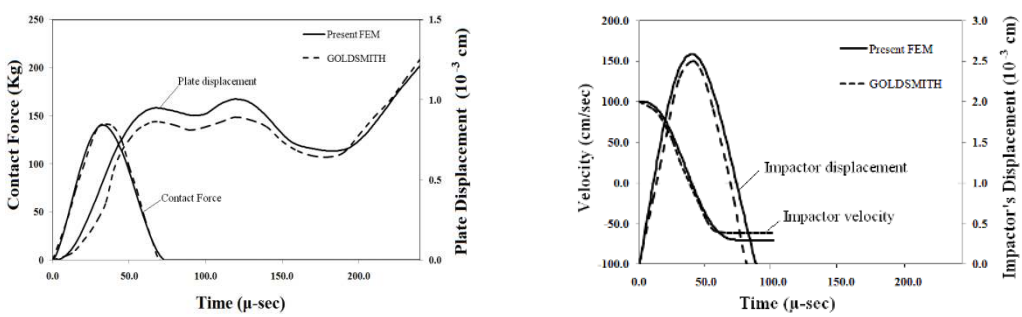


(a) (b)

Figure 4: (a) Contact force and plate displacement (b) Impactor's displacement and velocity with respect to time for simply supported plate impacted at the centre considering flat isotropic laminate with dimension a=b=20 cm, t=0.8 cm, time step=1.0 μ-sec, $E_1$=$E_2$=$E_i$=200 GPa, $G_{12}$=$G_{23}$=$G_{13}$=77 GPa, $\rho$= 7800 kg/m$^3$, $\nu_i$=$\nu_{12}$=0.3, initial velocity of impactor=1.0 m/s, radius of impact=0.01 m (Goldsmith, 1960).

The present analyses employed an eight noded plate bending element to portray the effect on functionally graded conical shells subjected to low velocity impact. Transient dynamic response is obtained for both untwisted ($\Psi$=0°) and twisted ($\Psi$=45°) Stainless steel – nickel functionally graded pretwisted shallow conical shells with both normal and oblique impact, using the converged value of time step of 1.0 μ-sec. At the impact point (L/2, b/2), contact parameters are obtained and the optimum value of time step is chosen after performing convergence study as furnished in Figure 6. In the present study, the dimensions of length (*Lo*), width (bo) and thickness (t) of the shells are adopted as 0.4 m, 0.06732 m and 0.002 m, respectively. Considering the complete planform of the conical shell a mesh division of (8 × 8) has been used for the analyses. For all the cases, conical shells are centrally impacted by a spherical steel ball of 0.0127 m diameter with different initial velocities. The material properties for computation are adopted as furnished in Table 1. Due to paucity of space, only a few important representative results are furnished.

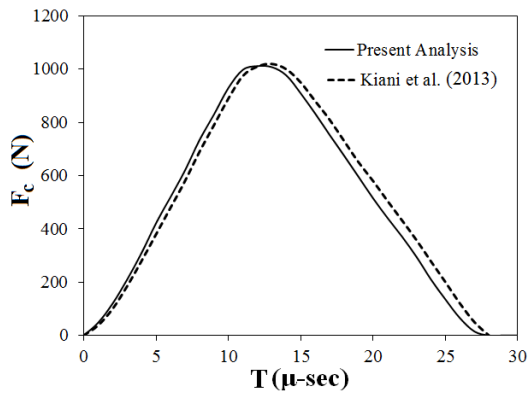


Figure 5: Time histories of contact force ($F_c$) for Silicon Nitride and Stainless Steel functionally graded beam clamped at both ends considering time step ($\Delta$t)=1.0 μ-sec, length (Lo)=135 mm, width (b)=15 mm, thickness (t)=10 mm, impactor of mass ($m_i$) = 0.01 Kg, radius of impactor ($r_i$) = 12.7 mm, velocity of impactor=1.0 m/s [Kiani et al. (2013)]

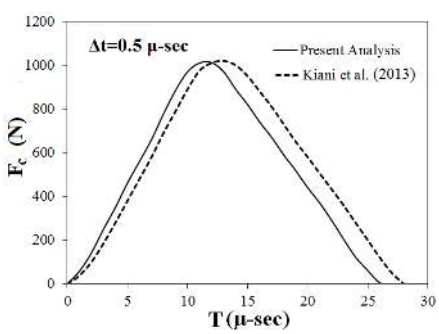


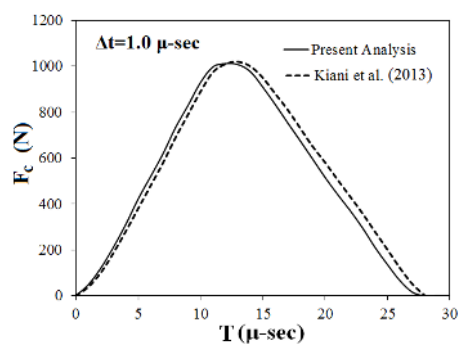

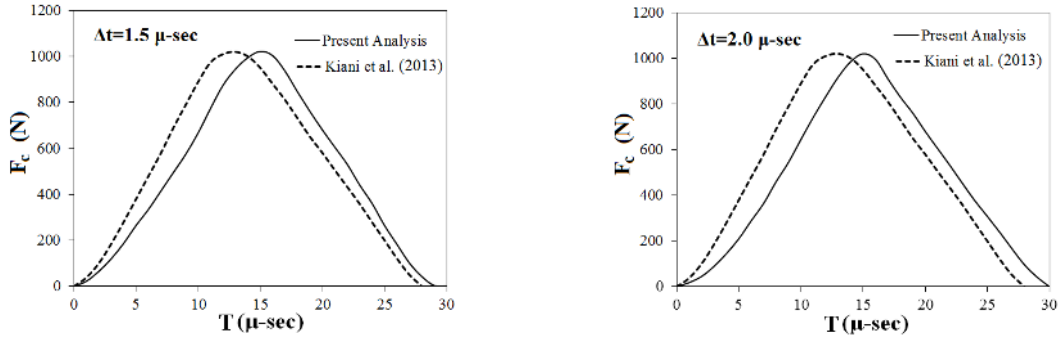


Figure 6: Time convergence study for histories of contact force ($F_c$) of Silicon Nitride and Stainless Steel functionally graded beam clamped at both ends considering length (Lo) =135 mm, width (b) =15 mm, thickness (t) =10 mm, impactor of mass ($m_i$) = 0.01 Kg, radius of impactor ($r_i$) = 12.7 mm, velocity of impactor=1.0 m/s [Kiani et al. (2013)].

### 5.1 Effect of initial velocity of impactor

The initial velocity of the impactor is an important factor affecting the impact process and design of an impact mitigation system. The effect of initial velocity of impactor is furnished in Figure 7. The peak value of contact force is found to increase with increase of initial velocity of impactor irrespective of twist angle. In contrast, the slope of deflection/thickness is found to reduce with the decrease of initial velocity of impactor. The impactor's displacement curve is observed to increase during loading and after reaching the peak value, it is found to decrease with a slope which is proportional to initial velocity of impactor. In this context, it is to be noted that the negative value of impactor's displacement indicates the situation when the impactor bounces back from target after the contact duration. For a particular value of initial velocity of impactor, the peak value of contact force of twisted cases is observed to be higher than that of untwisted cases. The contact duration has inverse relationship with initial velocity of impactor while the time at which peak value of contact force is achieved found to reduce with the increase of initial velocity of impactor. The unloading time for untwisted cases is observed to be higher than that of twisted cases while the contact force is found to increase invariably as the twist angle increases. Interestingly, it is to be noted that the contact force histories of three cases are identical in nature. Hence, the alternation of indentation is similar to the contact force with respect to initial velocity. This corroborates with the results obtained by Kaini et al. (2013). The time of peak value of contact force for twisted cases is obtained as higher than that of untwisted cases. In contrast, the total contact duration for untwisted cases is found to be higher than twisted cases irrespective of initial velocity of impactor. As the initial velocity of impactor increases, the total contact duration is found to reduce irrespective of twist angle. The slope of time history curves of velocity of impactor is found to be maximum value for VOI=10 m/sec, followed by VOI=5 m/sec and followed by VOI=1 m/sec. Interestingly the striker's velocity is observed to become a constant value at the end of unloading cycle (i.e., when the contact force dies down to null value) wherein the maximum constant value of velocity of impactor is found for VOI=1/sec and the minimum constant value of striker's velocity is obtained for VOI=10 m/sec

while the intermediate value of the same is observed at VOI=5 m/sec irrespective of twist angle. It is also to be noted that the velocity of the impactor dies down to null value at the end of contact duration and subsequently it drops down toward negative value wherein null value of contact force is observed.

### 5.2 Effect of material property graded index

The variation of properties profile is studied to enumerate its effect on impact parameters. It is observed that the impact parameters like contact force, deflection/thickness, impactor's displacement, velocity of the impactor with respect to time have variation with the rise of material property graded index for SS–Ni functionally graded shallow conical shells irrespective of twist angle. In other words, as the material property graded index increases, it is found to slightly increase the contact force and minutely reduce the contact duration of the loading-unloading cycle invariant to power law exponent. The time interval between completion of unloading and commencement of reloading is widened for cantilevered conical shells wherein the second impact does not occur within the time span of the analyses (e.g. 300 μ-sec). The contact duration for twisted cases is found to slightly lower than that of the same for untwisted cases irrespective of material property graded index or power law exponent (N). For a particular value of material property graded index, the peak value of contact force is found to intensify as the twist angle increases as furnished in Figure 8. This may be attributed to the fact that because of the coupling effects the increase of twist angle increases the elastic stiffness resulting in rise of maximum value of contact force. The time at which peak value of contact force is obtained and the total contact duration is found to be unaltered with the rise of material property graded index unless twist angle changes. Hence, it can be inferred that as the material property graded index increases, the indentation parameter increases which is expected since the functionally graded conical shell becomes softer as the material property graded index increases up.

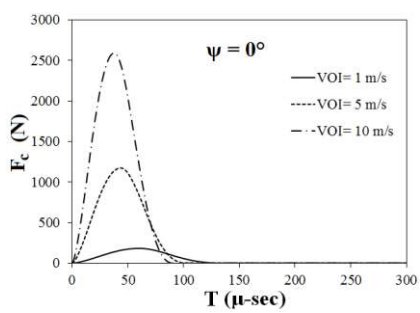


(a)

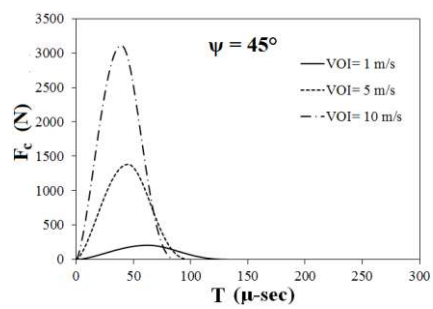


(b)

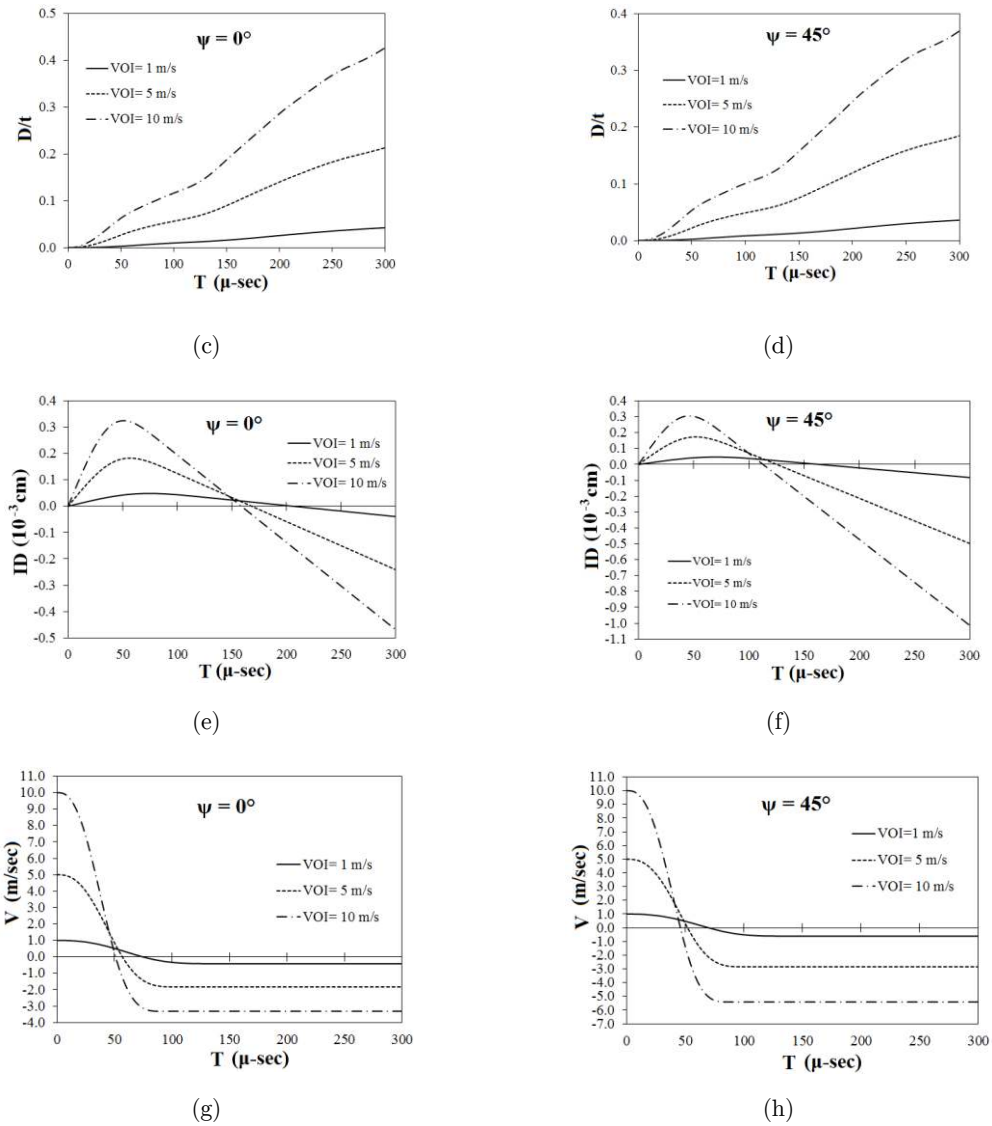


Figure 7: Effect of initial velocity of impactor on contact force ($F_c$), deflection/thickness (D/t), impactor's displacement (ID) and velocity of impactor (V) with respect to time (T) at $\psi$=0°, 45° for Stainless Steel Nickel functionally graded conical shells considering time step=1.0 μ-sec, N=1, t=0.002 m, L/s=0.7, $\phi_o$=45°, $\phi_{ve}$=20°.

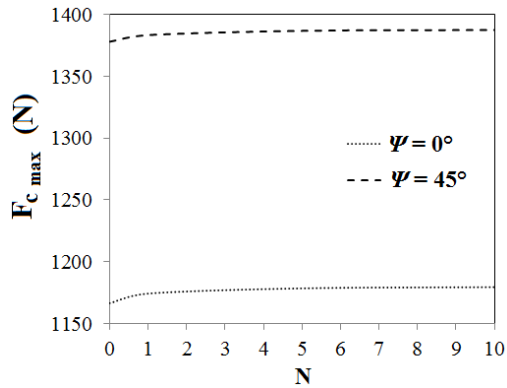


Figure 8: Variation of Peak value of contact force ($F_{c\ max}$) with material property graded index (N) at $\psi$=0°, 45° for pretwisted Stainless Steel Nickel functionally graded conical shells considering time step=1.0 μ-sec, N=1, t=0.002 m, L/s=0.7, $\phi_o$=45°, $\phi_{ve}$=20°.

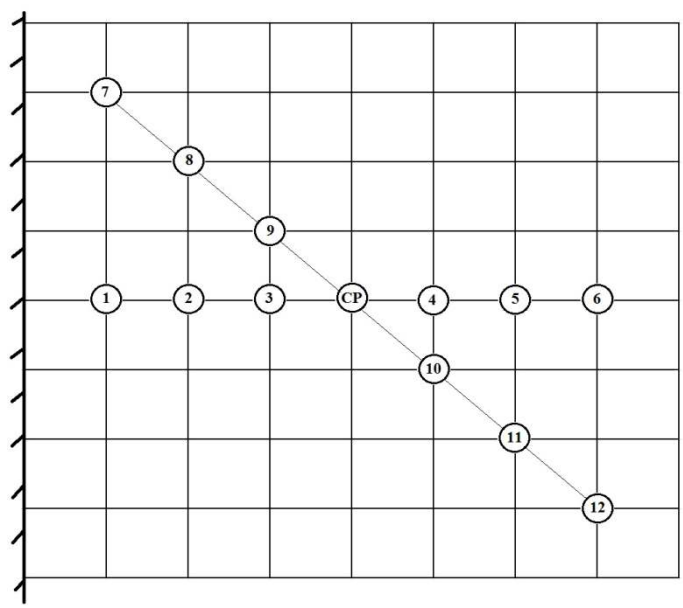


Figure 9: Location of impact (Spanwise and diagonal).

### 5.3 Effect of location of impact

The location point at which the spherical impactor hits the target i.e., functionally graded conical shell plays significant role as furnished in Figure 9 wherein the location of impactor is considered in both spanwise (Point 1-2-3-CP-4-5-6) and diagonal direction (Point 7-8-9-CP-10-11-12). Here CP denotes the central point of the conical shell. The variation of location of impact point is found to affect in the variation of effective elastic stiffness. Thus the peak value of the contact force is found to be maximum value at point 1 and minimum at point 6 along spanwise direction and for diagonal

direction, the maximum value of contact force obtained at point 7 and the lowest peak value of contact force is noted at point 12 as furnished in Figure 10. Hence, in case of spanwise direction (point 1 to point 6), the peak value of contact force is found to decrease as the point of impact moves from fixed end to free end of the functionally graded cantilever conical shells wherein the loading duration is found to increase from free end to fixed end. In contrast, the total contact duration is found to increase from fixed end to free end in spanwise direction. On the other hand, maximum value of contact force is obtained at fixed diagonal end (i.e, at point 7) and decreases as it moves diagonally from fixed end to free end wherein the total contact duration is found to increase from fixed end to free end diagonally (point 7 to point 12) while the unloading time duration is found to reduce from free end to fixed end. The slope of deflection/thickness with respect to time curve is observed to increase as it moves from fixed end to free end in both along spanwise and diagonal direction. The impactor's displacement with time is found to increase initially and after reaching the peak point it decreases and dies down from null or negative value along both spanwise and diagonal direction. The variation in peak value of contact force is found to be higher in diagonal direction compared to spanwise direction. Hence, it can be inferred that low velocity impact of FG conical shell in diagonal direction could be severe compared to the same along the spanwise direction. In other words, the FG conical shell subjected to low velocity impact which is safe in diagonal direction, subsequently becomes also safer in design along the spanwise direction.

### 5.4 Effect of oblique impact

The extent to which FG conical shell has been damaged can be calculated on the basis of contact force and displacement profile in that time interval. Evidence for this phenomenon is provided by the fact that after oblique impact, the strength of the SS-Ni functionally graded decreases. As a result, further loading and deflection may cause to severe damage in functionally graded conical shell structure. The time histories of the contact force, target displacement, impcator's displacement and velocity of impactor for SS-Ni functionally graded conical shells are furnished in Figure 11. In general, the peak value of contact force for untwisted SS-Ni functionally graded conical shells is always found to be lower than that of twisted cases irrespective of oblique angle. The percentage of difference between peak value of contact forces at twisted ($\Psi=45^\circ$) and untwisted ($\Psi=0^\circ$) SS-Ni functionally graded conical shells with N=1 are obtained as 19.8%, 20.0%, 21.7%, 22.1%, 24.7% and 30.5% corresponding to $\beta i=0^\circ$, $15^\circ$, $30^\circ$, $45^\circ$, $60^\circ$ and $75^\circ$ respectively. Hence it could be inferred that due to the coupling in twisted FG conical shell leads to higher structural stiffness thereby generating higher value of contact force irrespective of angle of oblique impact. As the angle of oblique impact increases, the peak value of contact force is found to reduce gradually and the lowest peak value of contact force is obtained at $\beta i=75^\circ$ irrespective of twist angle. In contrast, for $\Psi=45^\circ$ at $\beta i=0^\circ$, the peak value of contact force for functionally graded conical shell is found to be higher compared to the same value for untwisted case. The contact duration is also found to gradually increase as the angle of oblique impact ($\beta i$) increases from $0^\circ$ to $75^\circ$ in step of $15^\circ$. In conformity of the same, the time at which peak value of respective contact force obtained is also found to increase with the hike in oblique impact angle irrespective of twist angle. Interestingly at $\beta i=75^\circ$, the time at which contact force is obtained to die down after loading-unloading cycle at $\Delta t=219$ μ-sec for $\Psi=0^\circ$

and at $\Delta t$=229 μ-sec for $\Psi$=45° while the same at $\beta i$=0° is found at $\Delta t$=119 μ-sec for $\Psi$=0° and at $\Delta t$=114 μ-sec for $\Psi$=45°. During normal impact at N=1, the peak value of contact force is found to obtain at $\Delta t$=47 μ-sec for $\Psi$=0° and at $\Delta t$=50 μ-sec for $\Psi$=45° while the same at $\beta i$=75° is found at $\Delta t$=93 μ-sec for $\Psi$=0° and at $\Delta t$=102 μ-sec for $\Psi$=45°. The unloading duration for twisted cases are found to be higher than loading time of untwisted cases irrespective of oblique impact angle while the loading duration is observed to increase as the oblique impact angle increases irrespective of twist angle. On the other hand, the unloading time is found to be higher than loading time irrespective of twist angle and oblique impact angle. It is noted that the unloading time for twisted cases are found to be lower than the unloading time of untwisted cases irrespective of oblique impact angle. Total contact duration for untwisted cases is found to be higher than total contact duration for twisted cases irrespective of oblique impact angle and the contact duration is observed to increase with rise of oblique impact angle irrespective of twist angle.

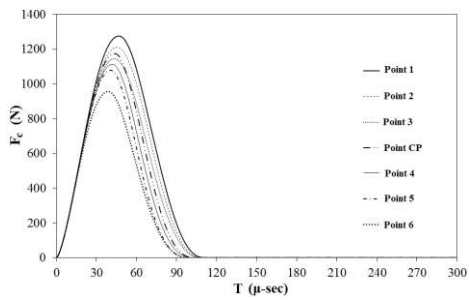


(a)

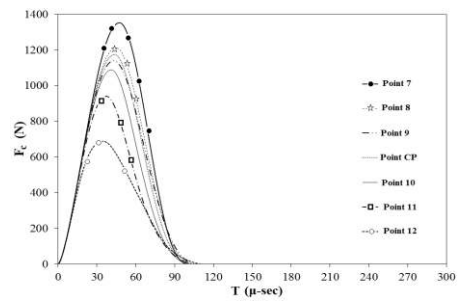


(b)

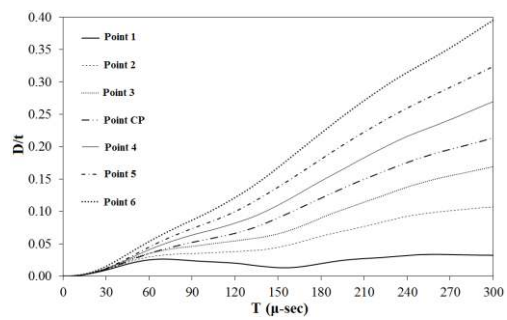


(c)

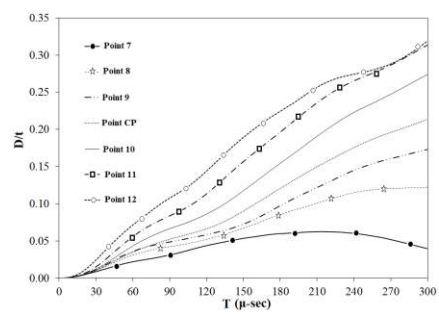


(d)

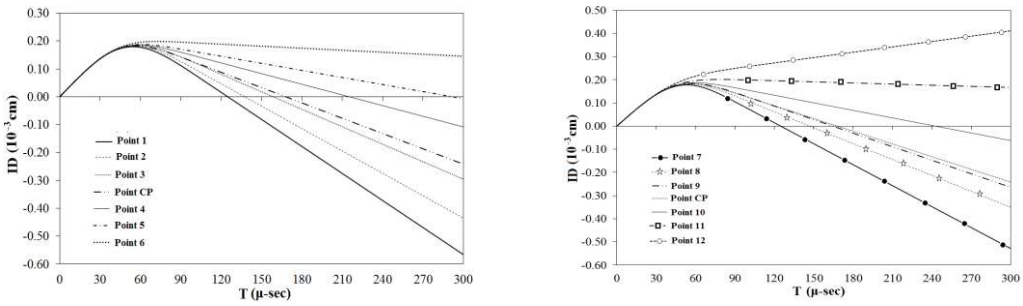


(e) (f)

Figure 10: Effect of loaction of impact on contact force ($F_c$), deflection/thickness (D/t) and impactor's displacement (ID) with respect to time (T) at $\psi$=0°, 45° for Stainless Steel Nickel functionally graded conical shells considering time step ($\Delta$t )=1.0 μ-sec, N=1, t=0.002 m, VOI=3 m/s, Lo/s=0.7, $\phi_o$=45°, $\phi_{ve}$=20°.

## 6 CONCLUSIONS

In the present investigation, the computer code is validated with the benchmark problems of open literature and hence this can be utilized to analyze the low velocity impact response of other type of functionally graded conical shells. For a particular value of material property graded index, the peak value of contact force is found to intensify as the twist angle increases but as the material property graded index increases, it is found to slightly increase the contact force and minutely reduce the contact duration irrespective of power law exponent. In general, the maximum value of contact force is found to increase with the rise of twist angle. As the angle of oblique impact increases, the peak value of contact force is found to reduce gradually and the lowest peak value of contact force is obtained at $\beta$i=75° irrespective of twist angle. In case of spanwise direction, the peak value of contact force is found to decrease as the point of impact moves from fixed end to free end of the functionally graded cantilever conical shells wherein the loading duration is found to increase from free end to fixed end. The results obtained are the first known results for the type of analyses carried out here.

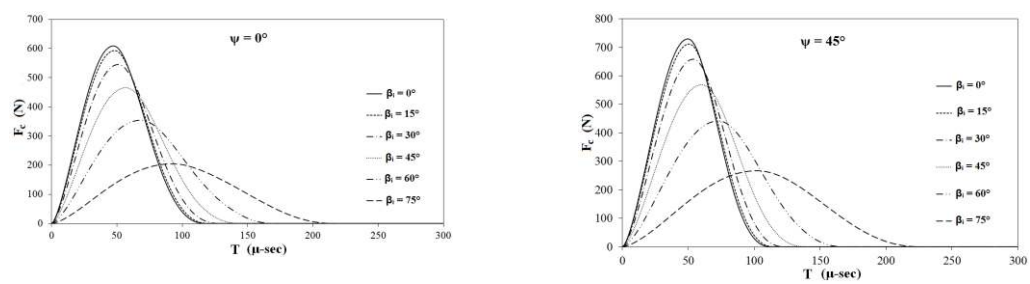


(a) (b)

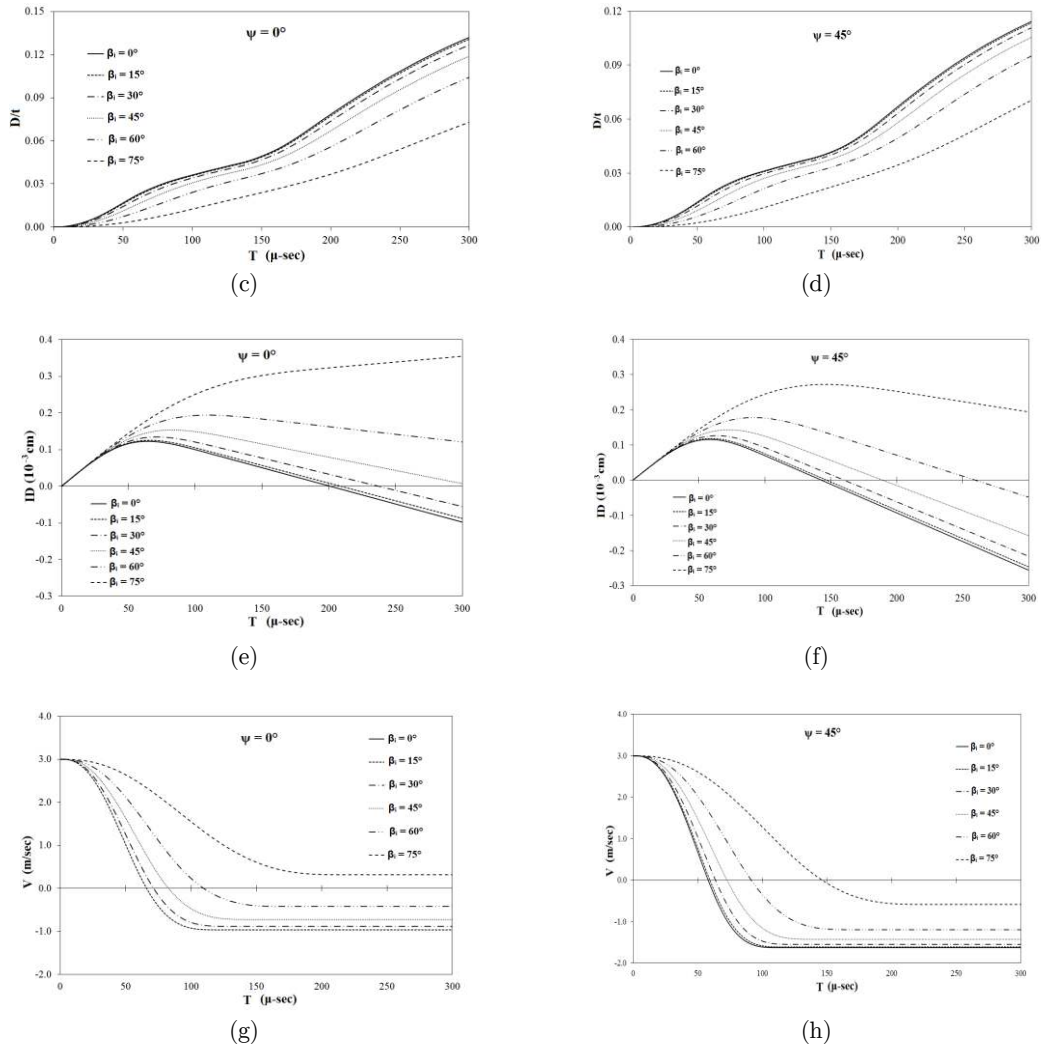


Figure 11: Contact force ($F_c$), deflection/thickness (D/t), impactor displacement (ID) and velocity of impactor (V) with respect to time (T) at $\psi$=0° and 45° for pretwisted Stainless Steel-Nickel functionally graded conical shells with different oblique impact angle ($\beta$i) considering time step ($\Delta$t)=1.0 μ-sec, N=1, $r_1$=0.2 m, VOI=3 m/s, Lo=0.8 m, t=0.002 m, L/s=0.7, $\phi_o$=45°, $\phi_{ve}$=20°.

## References

Abrate S., (1998). Impact on Composite Structures, New York: Cambridge University Press, 1998.

Amirhossein Nezhadi, Roslan Abdul Rahman, Amran Ayob, (2011). Transient Analysis of Functionally Graded Cylindrical Shell Under Impulse Local Loads, Australian J. of Basic and Applied Sciences, 5(12): 757-765.

Apetre N.A., Sankar V, Ambur, (2006). Low-velocity impact response of sandwich beams with functionally graded core, I. J. of Solids and Structures, 43(9): 2479-2496.

Bathe K. J., (1990). Finite Element Procedures in Engineering Analysis, New Delhi: PHI.

Dey S., Karmakar A., (2012). Free vibration analyses of multiple delaminated angle-ply composite conical shells – A finite element approach, Composite Structures, 94: 2188–2196.

Eghtesad A., Shafiei A.R., Mahzoon M., (2012). Study of dynamic behavior of ceramic–metal FGM under high velocity impact conditions using CSPM method, Applied Mathematical Modelling, 36(6): 2724-2738.

Etemadi E., Afaghi Khatibi A., Takaffoli M., (2009). 3D finite element simulation of sandwich panels with a functionally graded core subjected to low velocity impact, Composite Structures, 89(1): 28-34.

Fukui Y., Yamanaka N., Wakashima K. (1993). The stresses and strains in a thick-walled tube for functionally graded under uniform thermal loading. Int J Jpn Soc Mech Eng Ser A, 36: 156–62.

Goldsmith W., (1960). Impact: The theory and physical behaviour of colliding solids. E. Arnold P. Ltd., London

Gunes Recep, Aydin Murat, Apalak M. Kemal, Reddy J.N., (2014). Experimental and numerical investigations of low velocity impact on functionally graded circular plates, Composites Part B: Engineering, 59: 21-32.

Karmakar A., Kishimoto K., (2006). Transient dynamic response of delaminated composite rotating shallow shells subjected to impact, Shock and Vibration, 13: 619–628.

Karmakar A., Sinha P.K., (1998). Finite element transient dynamic analysis of laminated composite pretwisted rotating plates subjected to impact, I. J. of Crashworthiness, 3(4): 379-391.

Khalili S.M.R., Malekzadeh K., Gorgabad A. Veysi, (2013). Low velocity transverse impact response of functionally graded plates with temperature dependent properties, Composite Structures, 96: 64-74.

Kiani Y., Sadighi M., Salami Jedari S., Eslami M.R., (2013). Low velocity impact response of thick FGM beams with general boundary conditions in thermal field, Composite Structures, 104: 293-303.

Kubair D.V., Lakshmana B.K., (2008). Cohesive modeling of low-velocity impact damage in layered functionally graded beams, Mechanics Research Communications, 35(1–2): 104-114.

Larson R.A., Palazotto A. (2006). Low velocity impact analysis of functionally graded circular plates, In: Proceedings of IMECE 2006 ASME international mechanical engineering congress and exposition, Chicago, Illinois, USA, November 5–10, paper No.: IMECE2006-14003.

Liew K.M., Lim C.M., Ong L.S., (1994). Vibration of pretwisted cantilever shallow conical shells, I. J. Solids Structures, 31: 2463-74.

Loy C.T., Lam J.N., Reddy J.N., (1999). Vibration of functionally graded cylindrical shells, I.J. Mech. Sci, 41: 309-24.

Mao Yiqi, Fu Yiming, Ai Shigang, Fang Daining, (2013). Interfacial damage analysis of shallow spherical shell with FGM coating under low velocity impact, International Journal of Mechanical Sciences, 71: 30-40.

Mao Y.Q., Fu Y.M., Chen C.P.,. Li, (2011). Nonlinear dynamic response for functionally graded shallow spherical shell under low velocity impact in thermal environment, Applied Mathematical Modelling, 35(6): 2887–2900.

Meirovitch L., (1992) Dynamics and Control of Structures, J. Wiley & Sons, New York.

Noda N.,(1999). Thermal stresses in functionally graded materials, J. Thermal Stress, 22: 477–512.

Praveen G.N., Reddy J.N., (1998). Nonlinear transient thermoelastic analysis of functionally graded ceramic–metal plates, I. J. Solids and Structures, 33: 4457–76.

Shariyat M., Jafari R., (2013). A micromechanical approach for semi-analytical low-velocity impact analysis of a bidirectional functionally graded circular plate resting on an elastic foundation, Meccanica, 48: 2127–2148.

Shariyat M, Farzan F. (2013). Nonlinear eccentric low-velocity impact analysis of a highly prestressed FGM rectangular plate, using a refined contact law, Archive of Applied Mechanics, 83: 623-641.

Shariyat M., Farzan Nasab F., (2014). Low-velocity impact analysis of the hierarchical viscoelastic FGM plates, using an explicit shear-bending decomposition theory and the new DQ method, Comp. Struct., 113: 63-73.

Sun, C.T., Chen, J.K. (1985). On the impact of initially stressed composite laminates, Comp. Materials, 19: 490–504.

Yalamanchili V.K., Sankar B.V., (2012). Indentation of functionally graded beams and its application to low-velocity impact response , Composites Science and Technology, 72(16): 1989-1994.

Zhao X., Liew K. M, (2011). Free vibration analysis of functionally graded conical shell panels by a meshless method, Composite Structures, 93: 649–664.